

http://pubs.acs.org/journal/aesccq Article

Minimizing Errors in Measured Yields of Particle-Phase Products Formed in Environmental Chamber Reactions: Revisiting the Yields of β -Hydroxynitrates Formed from 1-Alkene + OH/NO_x Reactions

Julia G. Bakker-Arkema and Paul J. Ziemann*



Cite This: ACS Earth Space Chem. 2021, 5, 690-702



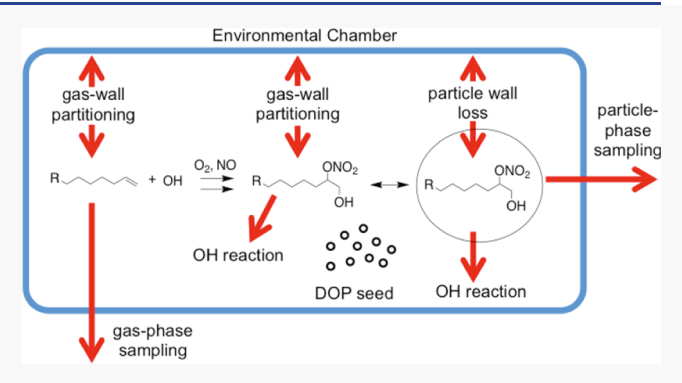
ACCESS I

III Metrics & More



S Supporting Information

ABSTRACT: Environmental chamber studies are widely used for measuring the yields of reaction products and secondary organic aerosol formed from the oxidation of volatile organic compounds, information that can be subsequently used to develop chemical reaction mechanisms and models of atmospheric chemistry. Such measurements are challenging, however, and many potential sources of errors are not always appreciated. Here, we describe methods for minimizing and accounting for uncertainties associated with the chamber volume, gas and particle sampling, instrument calibrations, gas—wall partitioning, particle deposition to walls, and secondary reactions with OH radicals and demonstrate these methods by measuring yields and branching ratios for the formation of β-hydroxynitrates from reactions of C_{14}



and C_{15} 1-alkenes with OH radicals in the presence of NO_x . Experiments were conducted in a Teflon environmental chamber and included Tenax sampling of alkenes with analysis by gas chromatography with flame ionization detection, filter sampling of particle-phase β -hydroxynitrates and dioctyl phthalate seed particles with analysis by liquid chromatography with UV/vis detection, and measurements of aerosol volume concentration and composition using a scanning mobility particle sizer and thermal desorption particle beam mass spectrometer. The measured yields of β -hydroxynitrates are \sim 25% higher than those determined previously using similar methods whose uncertainties were less well minimized and characterized.

KEYWORDS: atmospheric chemistry, volatile organic compounds, secondary organic aerosol, VOC oxidation, reaction mechanisms, product yields

■ INTRODUCTION

Volatile organic compounds (VOCs) are emitted into the atmosphere from biogenic and anthropogenic sources, with an estimated annual global budget of 1150 Tg for nonmethane VOCs. Biogenic VOCs predominately consist of alkenes, including isoprene (50%), monoterpenes (15%), and sesquiterpenes (3%), while anthropogenic VOCs consist of about 10% of alkenes.² In the atmosphere, alkenes can react with OH radicals, O₃, or NO₃ radicals to form more oxygenated products. β -Hydroxynitrates are important products of the oxidation of alkenes by OH radicals in the presence of NO_x. 4-9 For large alkene precursors, the addition of a hydroxyl group and a nitrate group to a carbon chain can sufficiently lower the vapor pressure such that products condense to form secondary organic aerosol (SOA),5,6 which can impact Earth's radiation budget10 and negatively influence visibility and human health.¹¹ For smaller alkenes, such as isoprene (the most abundant biogenic VOC), β -hydroxynitrates can serve as a sink for NOx, with implications for ozone formation and radical cycling.8,12,13

A number of studies have quantified yields of β -hydroxynitrates formed from a variety of simple linear and branched 1-alkenes and used these to determine branching ratios for β -hydroxynitrate formation. The mechanism for the reaction of 1-alkenes with OH radicals in the presence of NO is shown in Scheme 1, where the branching ratios for each reaction pathway (i) are labeled by α_i . The reaction is initiated by either addition of the OH radical to the C=C double bond or by abstraction of a H-atom along the carbon chain. As the length of the carbon chain increases, the percentage of reaction occurring by abstraction increases, but even for large alkenes, the reactivity is dominated by the OH radical addition to the C=C bond. For example, for a C₁₄ 1-

Received: January 9, 2021 Revised: February 13, 2021 Accepted: February 15, 2021 Published: February 25, 2021





Scheme 1. Abbreviated Mechanism for the Reactions of 1-Alkenes with OH in the Presence of NO_x, Where R Is an Alkyl Group

alkene, ~70% of the reaction occurs by addition.¹⁴ The OH radical adds to either of the carbon atoms to form a β hydroxyalkyl radical, which then adds O_2 to form a β hydroxyperoxy radical. In the presence of NO, the β hydroxyperoxy radical reacts with NO to form a β hydroxynitrate or a β -hydroxyalkoxy radical and NO₂. Subsequent decomposition or isomerization of the β hydroxyalkoxy radical leads to the formation of a variety of products, which are not the focus of this study and so are not shown in Scheme 1. We note that the β -hydroxyperoxy and β hydroxyalkoxy radicals can also react with NO₂ to form a β hydroxyperoxynitrate and β -hydroxynitrate, respectively, but the β -hydroxyperoxynitrate decomposes reversibly on a timescale of a few seconds¹⁵ (and therefore only acts as a short-term reservoir before the β -hydroxyperoxy radical eventually reacts with NO) and the $\sim 10^{-3}$ s timescale (1/ $k_{NO_2}[NO_2] = 1/(2 \times 10^{-11} \text{ cm}^3 \text{ molecule}^{-1} \text{ s}^{-116} \times 5 \times 10^{13}$ molecules cm⁻³)) for the reaction of β -hydroxyalkoxy radicals with NO_2 is much too long to compete with the $\sim 10^{-6}$ s timescales for decomposition and isomerization.¹⁷ The yields of β -hydroxynitrates increase with carbon number to a plateau due to enhanced stabilization of the β -hydroxyperoxy radical— NO complex.5,6,18

In spite of the need for accurate measurements of the yields and branching ratios for the formation of β -hydroxynitrates, there is currently a large discrepancy in reported values that is consistent over a range of carbon numbers. In particular, Teng et al. measured values that are about a factor of 2 larger than those measured by O'Brien et al. and Matsunaga and Ziemann and which are comparable to those that have been measured for similar reactions of n-alkanes. Each of these studies employed different methods to measure the β -hydroxynitrates, which seems to be the most likely source of the discrepancy, although chemical modeling by Teng et al. indicates that experimental conditions may have influenced the

results of O'Brien et al.⁴ O'Brien et al.⁴ used online gas chromatography with organic nitrate-specific chemiluminescence detection to measure gas-phase C_2-C_6 β -hydroxynitrates, Teng et al.⁷ used online gas chromatography-chemical ionization mass spectrometry and thermal dissociation-laser-induced fluorescence to measure gas-phase C_2-C_8 β -hydroxynitrates, and Matsunaga and Ziemann⁵ used filter sampling with high-performance liquid chromatography-UV/ vis detection to measure particle-phase $C_{14}-C_{17}$ β -hydroxynitrates and then extrapolated values to C_2 using a well-established model for the carbon number dependence of alkyl nitrate yields. ^{19,20}

In light of the importance of β -hydroxynitrates in atmospheric chemistry and significant unresolved discrepancies in previous measurements, we have thoroughly evaluated the methods used in our previous studies to measure yields and branching ratios for the formation of β -hydroxynitrates. This has led to a number of insights and recommendations that could benefit others measuring gas- or particle-phase products of VOC oxidation. Here, we describe the results and the identified sources of errors and their magnitudes using measurements of the yields of β -hydroxynitrates formed from the reactions of C₁₄ and C₁₅ 1-alkenes with OH/NO_x, although the described approaches can be applied to chamber studies of other reactions. These methods were then also used to determine the yields of β -hydroxynitrates formed from the reactions of 7-pentadecene, an internal alkene, and 2-methyl-1tetradecene, a branched alkene, with OH/NO_x.

EXPERIMENTAL SECTION

The chamber processes and analyses involved in the measurement of the molar yields (moles of product formed divided by moles of precursor reacted) of β -hydroxynitrates formed from the reaction of an alkene with OH/NO_x are shown in Figure 1. They include measurements of alkene and

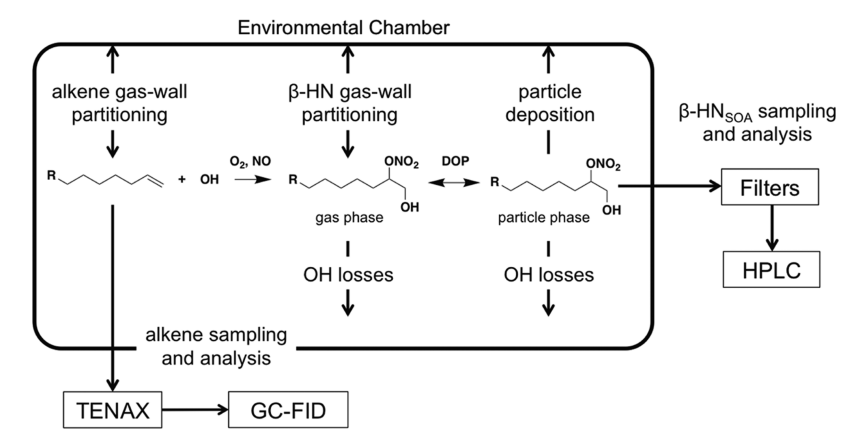


Figure 1. Experimental schematic demonstrating the processes and analyses involved in the determination of the yields of β-hydroxynitrates from reactions of alkenes with OH/NO_x.

 β -hydroxynitrate concentrations as well as determinations of losses to the chamber walls by gas—wall partitioning, particle deposition, and secondary reactions with OH radicals. Because the major focus of this report is to propose and demonstrate methods for optimizing the accuracy of measurements of the yields of products formed from reactions of VOCs in environmental chamber experiments, only a brief overview of the methods is provided in the Experimental Section. This is then followed by a detailed description of all of the important aspects of the methods in the Results and Discussion section.

Chemicals. These chemicals (with purities and suppliers) were used in this study: 1-octene (98%), 1-decene (94%), 1-tetradecene (96%), 1-pentadecene (98%), ethylhexyl nitrate (97%), dioctyl phthalate (99%), bis(2-ethylhexyl) sebacate (≥97%), acetonitrile (HPLC grade) [Sigma-Aldrich]; 7-pentadecene (95%), 2-methyl-1-tetradecene (99%) [ChemSampCo]; water (HPLC grade) [Fisher]; ethyl acetate (99.5%) [EMD Millipore]; CO_2 (99.5%), ultrahigh purity (UHP) N_2 and He [Airgas]; and NO (99.9%) [Matheson Tri Gas]. Isopropyl nitrite was synthesized using the procedure of Taylor et al. 21 for methyl nitrite and stored under vacuum.

Environmental Chamber Method. Reactions of 1tetradecene [CH₃(CH₂)₁₁CH=CH₂], 1-pentadecene $[CH_3(CH_2)_{12}CH=CH_2]$, 7-pentadecene $[CH_3(CH_2)_5CH=$ CH(CH₂)₆CH₃], and 2-methyl-1-tetradecene [CH₃(CH₂)₁₁C- $(CH_3)=CH_2$] with OH radicals in the presence of NO_x were performed in an ~7000 L FEP Teflon environmental chamber outfitted with blacklights on two walls and operated at room temperature (~25 °C) and atmospheric pressure (~84 kPa). The chamber was supplied with clean, dry air from two AADCO Model 737-14A clean air generators (<5 ppbv hydrocarbons, <0.1% RH). The timing of the various activities involved in conducting an experiment is shown in Figure 2. First, liquid dioctyl phthalate (DOP, a C₂₄ monoaromatic diester) aerosol seed particles, which are essentially nonvolatile, were added to the chamber from an evaporationcondensation apparatus to achieve a concentration of \sim 250 μg m^{-3} . This typically took ~ 30 min (period not shown in Figure 2) but could now be done in just a few minutes using a vaporizer we recently developed for generating organic seed particles in situ.²² A filter sample was then collected, and a measured amount of alkene was evaporated from an ~300 mL glass bulb (which was thoroughly heated using a heat gun and had a short outlet tube that was also kept hot to avoid condensation) and transported into the chamber in a stream of

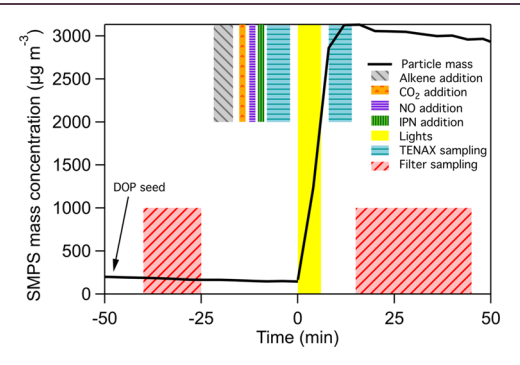


Figure 2. Time profile of aerosol mass concentration measured by the SMPS and representative time periods when alkenes, CO_2 , NO, and isopropyl nitrite (IPN) were added to the chamber (DOP seed particle addition is not shown); alkenes were sampled onto Tenax; filter samples were collected; and the lights were turned on to initiate reactions of the alkene with OH/NO_x .

UHP N_2 to achieve a mixing ratio of ~ 1 ppmv in the absence of gas-wall partitioning. Next, the chamber volume was determined by adding a known amount of CO₂ and measuring the change in the chamber concentration with a GMT 220 Series CO₂ probe. This was followed by the addition of sufficient NO and isopropyl nitrite to achieve mixing ratios of ~10 ppmv. These gases were added from a calibrated glass bulb (without heating) that was filled to the desired pressure on a vacuum manifold equipped with an MKS Baratron pressure gauge. A Teflon-coated fan was turned on for 15 s after the addition of each gaseous component to mix the chamber. Finally, alkenes were sampled onto Tenax solid adsorbent. The reaction was then initiated by turning on the blacklights for 6 min with an intensity equivalent to a NO₂ photolysis rate constant of ~0.14 min⁻¹ to generate OH radicals by isopropyl nitrite photolysis, which occurs according to the following reactions²

$$CH_3CH(ONO)CH_3 + h\nu \rightarrow CH_3CH(O)CH_3 + NO$$
 (1)

$$CH_3CH(O)CH_3 + O_2 \rightarrow HO_2 + CH_3C(O)CH_3$$
 (2)

$$HO_2 + NO \rightarrow OH + NO_2$$
 (3)

with the added NO serving to suppress the formation of O_3 and NO_3 radicals. One experiment was also conducted with the blacklights on for only 1 min, but with the intensity

equivalent to a NO₂ photolysis rate constant of 0.57 min⁻¹. After the lights were turned off, alkenes were again sampled onto Tenax solid adsorbent and particles were again collected on filters. Throughout experiments, the particle volume concentration and composition were monitored in real time using a scanning mobility particle sizer (SMPS)²⁴ and thermal desorption particle beam mass spectrometer, 25 respectively, and NO and NO, mixing ratios were measured with a Thermo Environmental Instruments 42D NO-NO₂-NO_r analyzer. Tenax samples were analyzed by gas chromatography with flame ionization detection (GC-FID) to determine alkene concentrations, and filter samples were extracted and analyzed by high-performance liquid chromatography with UV/vis detection (HPLC-UV/vis) to determine DOP and β hydroxynitrate concentrations. Typically, ~40 to 50% of the alkene reacted, aerosol mass concentrations increased to a maximum of $\sim 3000 \ \mu g \ m^{-3}$ within a few minutes, NO mixing ratios remained above 6 ppmv, and NOx mixing ratios were approximately constant. The experimental conditions are given in Table S1.

■ RESULTS AND DISCUSSION

The molar yield of β -hydroxynitrates formed from the reaction of an alkene is equal to the moles of β -hydroxynitrates formed divided by the moles of alkene reacted. To accurately measure the yield, it is necessary to sample and measure concentrations of alkenes and β -hydroxynitrates with as little error as possible and to correct these measurements for losses that might occur during the reaction, sampling, or analysis (Figure 1). For the alkene, this means accurately measuring the chamber volume, developing accurate calibrations for GC-FID analysis, minimizing losses to tubing walls and from breakthrough during Tenax sampling, and accounting for gas-wall partitioning to the chamber walls during an experiment. For the β -hydroxynitrates, this means minimizing losses of particles inside the filter sampling apparatus, minimizing losses of particles by deposition to the chamber walls, developing accurate calibrations for HPLC-UV/vis analysis, and accounting for gas-wall partitioning, secondary reactions with OH radicals, and particle deposition to the chamber walls. The approach used here was to evaluate our methods by quantifying the yields of β -hydroxynitrates formed from reactions of OH/NO_x with the C_{14} and C_{15} 1-alkenes, 1-tetradecene (1-TD), and 1pentadecene (1-PD), in eight experiments (four each), and then use the same methods for single experiments with 7pentadecene (7-PD) and 2-methyl-1-tetradecene (2M-1-TD). The results of the experiments are described in the following sections, and since the goal of the study was to develop methods to minimize and quantify as many sources of errors as possible, these aspects of the approach are discussed in detail.

Measurement of the Amount of Alkene Reacted. This measurement requires a measurement of the chamber volume, Tenax sampling and GC-FID analysis of the alkene, and determination of the loss of the alkene to the chamber walls by gas—wall partitioning.

Chamber Volume. The volume of an environmental chamber can be estimated from its dimensions; however, this is only reasonable for rigid chambers. For chambers constructed with a flexible material, such as commonly used FEP or PFA Teflon film, ²⁶ the volume will depend on the degree of inflation. Because the state of such a chamber can be difficult to reliably reproduce, the chamber volume should be directly measured before each experiment. Here, the chamber

was first thoroughly examined for leaks 24 h prior to each experiment. The volume of the chamber was then determined immediately after adding the alkene by filling a 2.059 L glass bulb with ~84 kPa of CO₂ on the vacuum manifold and then flushing into the chamber with a stream of UHP N₂. The mixing ratio of CO₂ in the chamber was monitored with a GMT 220 Series CO₂ probe, which was inserted directly into the chamber through a sealable Swagelok port. The probe measures the CO₂ concentration and then reports values as a mixing ratio at 84 kPa, the ambient pressure in Boulder, CO, where 1 ppmv = 2.04×10^{13} molecules cm⁻³. The probe was calibrated using mixtures of CO2 in zero air with mixing ratios ranging from 0 to 1000 ppmv. Mixtures were prepared on the vacuum manifold, and because of the high accuracy of the MKS Baratron pressure gauge ($\pm 0.25\%$ of reading), the mixing ratios should be accurate to $\pm 1\%$. The resulting calibration curve is shown in Figure S1. The amount of CO2 added to the chamber was selected so the resulting mixing ratio would be approximately twice that of chamber air and so the difference could be easily measured. The chamber volume was calculated using the equation

$$V_{\rm C} = V_{\rm B} P_{\rm B} / \Delta P_{\rm C} \tag{4}$$

where $V_{\rm C}$ and $V_{\rm B}$ are the chamber and bulb volumes and $P_{\rm B}$ and $\Delta P_{\rm C}$ are the CO₂ pressure in the bulb and the change in CO₂ partial pressure in the chamber, respectively. An example time profile of CO₂ in the chamber measured before and after adding CO₂ and mixing the air is shown in Figure 3, where it

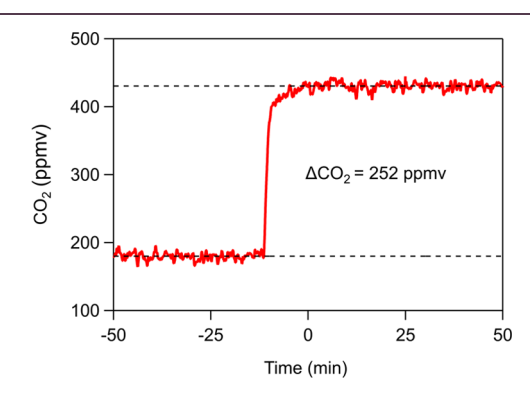


Figure 3. Representative time profile of chamber CO_2 concentrations used to calculate the chamber volume. The dashed lines are averages measured before adding CO_2 and then after adding CO_2 and mixing the chamber.

should be noted that the CO_2 mixing ratio in air from the Aadco clean air systems is less than in ambient air. The values for V_B , P_B , and ΔP_C of 2.059 L, 78.3 kPa, and 2.11 \times 10⁻² kPa (252 ppmv \times 84 kPa), respectively, yield a chamber volume of 7640 L. The measured chamber volume ranged from 6280 to 7640 L in eight experiments, with an average of 6930 \pm 540 (Table S1). This result confirms that it can be difficult to ensure that the chamber is inflated to the same degree in each experiment and indicates that using the average volume rather than individually measured chamber volumes could introduce errors of \pm 9% in measured product yields.

Tenax Sampling of Alkenes. The alkene was added to the chamber as described above. Addition took \sim 5 min, followed by \sim 15 s of mixing, and the alkene was allowed to equilibrate with the chamber walls for \sim 20 min. Three sequential 2 min Tenax samples were then collected for GC-FID analysis of the

alkene, the lights were turned on for 6 min, and then three more 2 min samples were collected. The time periods for alkene addition and Tenax sampling are shown in Figure 2. Prior to collecting each set of Tenax samples, the PFA Teflon sampling line was passivated (equilibrated with the alkene concentration in the chamber) by pulling chamber air for 1 min at 250 cm³ min⁻¹ using a Tylan mass flow controller. Our previous studies²⁷ have shown that the time required to passivate the 10 cm long, 0.635 cm OD, 0.476 cm ID tube for sampling any of these alkenes is <50 s. Immediately after passivation, the three Tenax samples were collected at the same flow rate by pulling the chamber air through a 10 cm long, 0.635 cm OD, 0.4 cm ID glass tube packed with 3 cm of Tenax held between glass wool plugs, resulting in a 6 min sampling time for each set of measurements. Measurements using two Tenax tubes in series verified that there is no alkene breakthrough under these sampling conditions. Tenax samples were stored in sealed glass tubes before and after sampling until analysis.

GC-FID Analysis of Alkenes. Tenax samples were analyzed within 24 h of collection using a Hewlett-Packard HP 6890 GC-FID instrument equipped with a 30 m \times 0.53 mm Agilent DB-1701 column with a 1 μ m film thickness. The Tenax tube was inserted into the inlet, where the alkene was thermally desorbed at 250 °C. The column temperature was maintained at 40 °C for 7 min and then increased linearly at a rate of 10 °C min⁻¹ to 280 °C, where it was held for another 10 min. The carrier gas was UHP He supplied at a flow rate of 1 mL min⁻¹.

Loss of Alkenes by Gas-Wall Partitioning. The measured yields of β -hydroxynitrates can be influenced by partitioning of the alkene to the Teflon chamber walls, a process that occurs reversibly for VOCs on time scales of ~ 10 to 60 min.²⁸⁻³¹ To evaluate the partitioning of alkenes to the chamber walls, an experiment was conducted with a mixture of 0.5 ppmv each of 1-octene, 1-decene, 1-tetradecene, and 1-pentadecene. 1-Alkenes were added to the chamber in ~5 min (as normal), and then 2 min Tenax samples were taken 1, 4, 10, 15, 25, and 45 min later. The time profiles of GC-FID signals are shown in Figure 4A, where signals have been normalized to the values expected in the absence of gas-wall partitioning and t = 0 is the time when the addition of 1-alkenes begins (since this is also when partitioning to the walls begins). For 1-octene and 1-decene, the expected signals for each at t = 0 were taken to be the average signal from all six samples (values agree within $\pm 2\%$) since these compounds are too volatile to partition to the chamber walls.²⁴ For 1-tetradecene and 1-pentadecene, the average signals from each of the six samples (values agree within ±3%) fall below the expected linear relationship between the added 1-alkene mass concentration and GC-FID signal (Figure 4B) due to partitioning to the chamber walls. Expected signals for these 1-alkenes at t = 0 in Figure 4A were therefore calculated from the extrapolated portion of the curve shown in Figure 4B. The curves in Figure 4A indicate that (within measurement uncertainties) 1-tetradecene and 1pentadecene reached partitioning equilibrium in ~10 to 20 min, at which time \sim 12 and \sim 17% had partitioned to the walls.

In the eight experiments measuring yields of β -hydroxynitrates from reactions of 1-tetradecene and 1-pentadecene, the three 2 min alkene Tenax samples collected beginning 7, 5, and 3 min before reaction and 3, 5, and 7 min after reaction agreed within $\pm 5\%$ and showed no consistent upward or downward trend, indicating that the 1-alkenes were essentially in equilibrium with the chamber walls (and sampling lines)

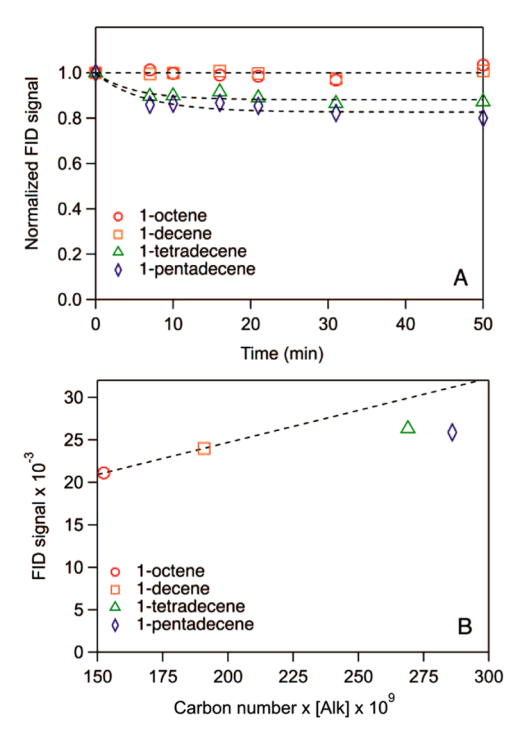


Figure 4. (A) Time profiles of GC-FID measurements of 1-alkenes added to the environmental chamber and allowed to partition to the walls. For 1-tetradecene and 1-pentadecene, the dashed curves are least-squares fits to the exponential function $A_t = A_{\infty} + (A_o - A_{\infty}) e^{-t/\tau}$, where A is the fraction of the 1-alkene in the gas phase, while for 1-octene and 1-decene, the dashed lines are averages of all data points collected. The signals were all normalized to the values expected at t=0 before any partitioning occurred, which for 1-octene and 1-decene were the measured signals and for 1-tetradecene and 1-pentadecene were the signals obtained by extrapolating the calibration curve in panel (B). (B) Calibration curve used to determine the signal expected if added 1-alkenes were present entirely in the gas phase. The data point for each alkene is the average of the six measurements in (A) after t=0.

when sampled before and after the reaction. It should be remembered that in these experiments only the small fraction of 1-alkene that was present in the walls before the reaction needed to re-partition to establish equilibrium (unlike the partitioning experiment discussed above) and that this began as soon as the reaction began, 9-16 min before the Tenax samples were collected. The average fractions of 1-tetradecene and 1-pentadecene that partitioned to the walls at equilibrium before the reaction were 7 ± 2 and $17 \pm 4\%$, respectively, consistent with the partitioning experiment described above and our previous measurements.²⁸ The concentration of 1-alkene reacted was then calculated using the equation

$$[Alk]_{reacted} = ([Alk]_{T,i}/FID_i)(FID_i - FID_f)$$
$$= [Alk]_{T,i}(1 - FID_f/FID_i)$$
(5)

where $[Alk]_{T,i}$ is the mass of 1-alkene added divided by the chamber volume, and FID_i and FID_f are the FID signals divided by the sampled volume of air before and after reaction. This equation is valid when no gas—wall partitioning occurs or when 1-alkenes are at gas—wall partitioning equilibrium before and after the reaction since in that case the same partitioning coefficients are used to correct the FID signals for the fraction of 1-alkene partitioned to the walls and these cancel out of the

equation.²⁰ Use of this equation has the advantage of not requiring a calibration curve like that shown in Figure 4B to quantify the amount of 1-alkene that reacted.

Measurement of the Amount of β-Hydroxynitrate Formed. This measurement requires filter sampling and HPLC analysis of the β-hydroxynitrates and determination of the loss of β-hydroxynitrates by deposition of particles to the chamber walls, gas—wall partitioning, and secondary reactions with OH radicals.

Filter Sampling of β -Hydroxynitrates. Duplicate samples of aerosol particles were collected in parallel twice during each experiment, as shown in Figure 2. One pair was collected for 15 min beginning \sim 30 min prior to initiating the reaction, when the only aerosol in the chamber was dioctyl phthalate (DOP) seed particles. Then, immediately following the reaction, another pair of samples was collected for 30 min. The relatively short sampling time compared to our previous studies^{5,6} minimized the corrections made for particle wall loss, as described below. Particle samples were collected in parallel on Millipore Teflon filters (0.45 μ m pore size, Fluoropore PTFE, 47 mm), with flows controlled using critical orifices calibrated using a Sensidyne Gilibrator. Flow rates were 13.6 \pm 0.2 and 14.3 \pm 0.2 L min⁻¹ for the two samplers and did not change during sampling since the pressure drop across filters remained constant at 1.5 kPa. Following sample collection, filters were immediately extracted three times with 4 mL of ethyl acetate for >10 min and then the extracts were combined. In one experiment, two filters were placed in the filter holder to test for breakthrough, and the amount collected on the back-filter was 1% of the total. This might have been due to particle breakthrough or condensation of vapor, but since the fraction was so small, it was assumed that the collection efficiency for a single filter was 100%. In another experiment, the sampling line (20 cm long, 0.635 cm OD, 0.476 cm ID stainless steel tube) and filter holder were evaluated for particle losses to surfaces by extracting the entire apparatus for comparison with the filters. Particle losses were <2% (consistent with theoretical estimates predicting negligible deposition due to inertial impaction or diffusion)³² and thus were assumed to be negligible in subsequent experiments. The filter extraction efficiency calculated by comparing the extracted mass to the mass determined by weighing the filters was 99.6 \pm 3% for the eight experiments and so was assumed to be 100%.

We note that in our previous studies 5,6 that employed this filter sampling apparatus, perforated metal screens provided by the manufacturer were placed over the filters (presumably to support the filter in the event of backpressure), and unfortunately were not extracted. Particle deposition to the screens was therefore investigated in three experiments (Table S1, expt 1–3) by extracting the screens along with the filters, with the results indicating that the screens collected $19 \pm 3\%$ of the total particle mass. For the other experiments, the screens were removed, and no significant difference was observed in the results of all eight experiments (Table S1). All else being equal, the improved particle sampling method should increase the yields of particle-phase reaction products measured here by $\sim 19\%$ compared to Matsunaga and Ziemann. 5,6

HPLC Analysis of β-Hydroxynitrates. Filter extracts were analyzed using a Shimadzu Model 20A HPLC equipped with a Zorbax 5 μ m XDB-C18 column coupled to a UV/vis diode array detector. Adequate separation was achieved using a

water/acetonitrile gradient elution method that increased from 50% acetonitrile to 100% over 60 min. Compounds containing a nitrate group were detected at 210 nm, where the molar absorptivity of nitrate-containing compounds is 20 or more times greater than that of the other functional groups present in the SOA (alcohols, carboxylic acids, ketones, and alkenes), 33 while DOP was monitored at 275 nm.

An example chromatogram is shown in Figure 5A. The β -hydroxynitrates, which had previously been identified from

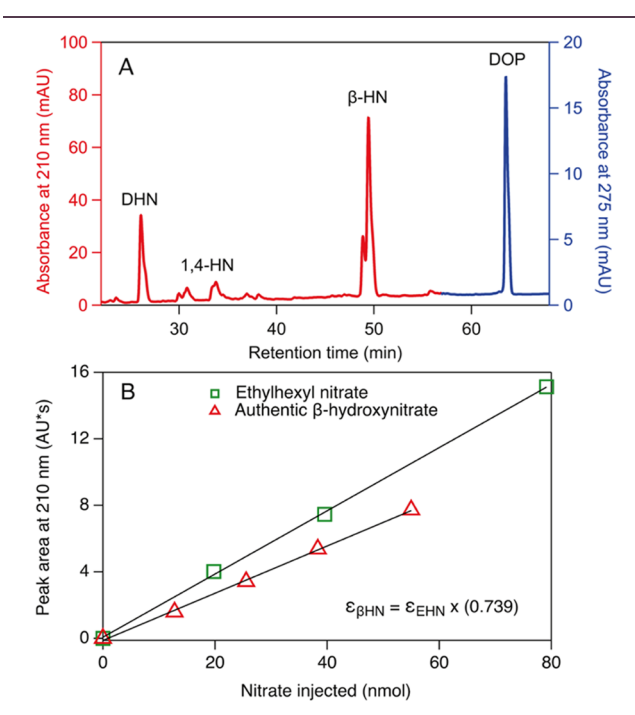


Figure 5. (A) HPLC–UV/vis chromatogram of SOA formed from the reaction of 1-tetradecene with OH/NO_x. The absorbance of nitrates and DOP was measured at 210 and 275 nm, respectively. (B) Calibration curves for a synthesized C_{14} β -hydroxynitrate standard and ethylhexyl nitrate.

their EI mass spectra obtained by coupling the HPLC to the TDPBMS and confirmed by $\mathrm{H}^1\text{-}\mathrm{NMR}$ analysis, were identified by their HPLC retention times, which matched those from our previous study. Two additional hydroxynitrate products, dihydroxynitrates (DHN) formed by the OH radical addition pathway and 1,4-hydroxynitrates (1,4-HN) formed by the H-atom abstraction pathway, are also shown in the chromatogram but were not quantified. Although they both absorb at 210 nm, they could be distinguished from the β -hydroxynitrates by their retention times and so did not contribute to the measured β -hydroxynitrate yields.

The β -hydroxynitrates were quantified by comparing the measured absorbance to the calibration curve shown in Figure 5B, which was prepared with an authentic β -hydroxynitrate standard. This standard was obtained by fractionating an SOA extract from the 1-tetradecene reaction on the HPLC using a semipreparative column (9.4 mm \times 250 mm Zorbax Eclipse EDX-C18) and then collecting fractions containing a mixture of the β -hydroxynitrate isomers (1-hydroxy-2-nitrooxy and 1-nitrooxy-2-hydroxy tetradecane). Also, in one experiment, fractions of the background mobile phase that eluted immediately before and after the β -hydroxynitrate peaks were collected for a period equal to the elution time for the β -hydroxynitrates to determine the mass of nonvolatile

components present in the solvent. Fractions were dried under a stream of UHP N_2 and weighed on a Mettler Toledo XS3DU Microbalance, which has a stated accuracy of $\pm 1~\mu g$. The mass of β -hydroxynitrate collected was 88 μg , while the mass of nonvolatile components in the HPLC solvent was <1 μg and therefore negligible. The calibration curve shown in Figure 5B was then created by preparing a 1.28 mM solution of the β -hydroxynitrate standard in acetonitrile and injecting 0, 10, 20, 30, and 40 μ L into the 100 μ L injection loop of the HPLC. A similar curve was prepared for DOP using the commercial standard.

This approach to generating an authentic β -hydroxynitrate standard curve addressed an important challenge for quantifying products formed in environmental chamber experiments since there is a general lack of commercially available standards for most multifunctional reaction products. For this reason, surrogate standards with similar chemical properties and functional groups are often used instead. However, in UV/vis measurements, the presence of other functional groups on the carbon backbone, especially within close proximity to the chromophore (such as the hydroxyl group adjacent to the nitrate group), can significantly alter the molar absorptivity of a compound.³⁴ For example, Figure 5B also shows the calibration curve for a possible organic nitrate surrogate, commercially available ethylhexyl nitrate, for comparison with that of the authentic C_{14} β -hydroxynitrate standard. The ratio of the molar absorptivity of the C_{14} β hydroxynitrate standard relative to ethylhexyl nitrate was 0.739. Since the product concentration is calculated by dividing the measured absorbance by the molar absorptivity, this indicates that the use of ethylhexyl nitrate to quantify the β-hydroxynitrate products would have caused a 35% underestimation in the β -hydroxynitrate yield. We also note that the ratio of 0.739 measured here is slightly smaller than the value of 0.786 reported by Matsunaga and Ziemann, indicating that the use of the value determined here would increase β hydroxynitrate yields by 6%.

It should also be emphasized that accurate mass measurements were critical for the preparation of the β -hydroxynitrate calibration curve. The accuracy of the microbalance used in our previous experiments^{5,6} was not known (it was located in another research lab), but the 6% agreement between the ratios of the molar absorptivity of the C_{14} β -hydroxynitrate standard relative to ethylhexyl nitrate measured here and previously indicates that previous mass measurements were quite accurate. Here, the calibration of the microbalance was regularly checked by comparing the readout with deposited known masses of bis(2-ethylhexyl) sebacate (commonly called dioctyl sebacate, DOS), a nonvolatile C26 diester. For those measurements, a 1.00 g L⁻¹ solution of DOS in ethyl acetate was prepared and then 10, 20, 30, 40, and 50 μ L aliquots were added to five preweighed metal boats that weighed \sim 200 μ g when empty. The mass per uL of solvent residue was also determined by adding 20 μ L of ethyl acetate to a boat. The solvent was then evaporated from each boat in a stream of UHP N2 and the boats were reweighed. The mass deposited in each boat was calculated from the volume of solution deposited and the concentrations of the DOS solution and ethyl acetate residue of 1.00 and 0.005 g L⁻¹ and the density of DOS, 0.912 g cm⁻³. A plot comparing the deposited and measured mass is shown in Figure S2. Since all values agreed within ±2% and were randomly scattered about the 1:1 line,

the microbalance readout was assumed to be accurate in all measurements.

Loss of β -Hydroxynitrates by Particle Deposition to Chamber Walls. Another factor that influences measured yields of particle-phase products in environmental chamber studies is particle wall loss.³⁵ Particles deposit to chamber walls at rates that depend on particle size, and when the particles and Teflon chamber walls are charged, the rates of particle wall loss will increase (one should thus avoid contacting chamber surfaces to prevent buildup of electrostatic charge). There are many methods of correcting for particle wall loss, including measuring loss rates of an inert seed in seed-only experiments, size-dependent SMPS measurements, semiempirical SMPS methods, methods employing aerosol mass spectrometer measurements of organic and sulfate seed ions, and use of aerosol dynamics models. In this study, DOP particles were used both as seeds and as an internal standard since the presence of a chromophore (an aromatic ring) in the DOP allows for quantification by HPLC with UV/vis detection at the same time as the β -hydroxynitrates (Figure 5A). A representative time profile of the volume concentration measured with the SMPS and the filter collection times is shown in Figure 2. The first filter sample was collected before the reaction when the chamber contained only DOP particles. DOP concentrations determined from HPLC analysis of filter extracts agreed with filter mass measurements to within ±4% for all experiments. Results of HPLC analyses were used to determine the ratio of the DOP mass concentration at the beginning of the reaction, [DOP], relative to the concentration of DOP measured in the chamber during the 30 min filter sampling period after reaction, [DOP]_f, and then this ratio was multiplied by the measured amount of β hydroxynitrates to correct for loss of particles to the walls during filter sampling. We note that filter mass measurements were consistently ~25% higher than those calculated from the average aerosol volume concentration measured with the SMPS during the sampling period and a DOP density of 0.985 g cm⁻³, falling within the combined uncertainties reported in SMPS evaluations.³⁶ This discrepancy was confirmed in separate experiments in which $\sim 250 \ \mu g \ m^{-3}$ of DOP seed particles was added to the chamber. Filters were collected for 30 min and weighed to determine an average correction factor for the SMPS of 1.24 \pm 0.06 for six experiments.

This particle deposition correction approach only assumes that the particle-phase β -hydroxynitrates were lost to walls at the same rate as the DOP and had the advantage that the DOP and β -hydroxynitrates were sampled and measured by the same methods. Although the correction method does not incorporate the effects of particle size on wall loss rates, because the particles were >200 nm throughout an experiment, this effect should be negligible. For the eight experiments, the particle wall loss ranged from 2.1 to 7.1%, with an average of 5.0 \pm 2% for the 30 min sampling period, similar to values determined from SMPS measurements (~4% in Figure 2) and to those reported by others. The 30 min sampling time used here significantly reduced the correction for particle wall loss compared to the 2 h periods we used previously. Figure 3.

Loss of β -Hydroxynitrates by Gas–Wall Partitioning. As with the alkenes, β -hydroxynitrates that are present in the gas phase might partition to the walls during an environmental chamber experiment, leading to an underestimate of the yields. In our previous study of the yields of β -hydroxynitrates formed from reactions of C_8 – C_{17} 1-alkenes, 5 we observed that the

total isomer yields determined from filter samples increased from ~ 0 for C_8 to a plateau at C_{14} . Although there was an indication that the 1-nitrooxy-2-hydroxy isomer (the minor isomer) did not reach a plateau until C₁₆, the variation for $C_{14}-C_{17}$ was within measurement uncertainties and so was most likely due to small errors in the assignment of the HPLC peak area to the two isomers, which were not fully resolved. The increase in yield with carbon number was due to the enhanced gas-to-particle partitioning as the vapor pressures of the β -hydroxynitrates decreased, with the results clearly showing ~100% partitioning to particles at the plateau. The trend is consistent with predictions of the gas-particle partitioning theory³⁷ and timescales for reaching partitioning equilibrium.²⁸ For example, using vapor pressures calculated with the SIMPOL.1 group contribution method³⁸ and a DOP seed particle mass concentration of 250 μ g m⁻³ at the beginning of the reaction, it is predicted that C_{14} β hydroxynitrates are ~94% in the particles and that partitioning equilibrium is reached in ~10 s. As the aerosol mass increases to $\sim 3000 \ \mu g \ m^{-3}$ at the end of the reaction (Figure 2), the fraction in the particles increases to >99% and the equilibration timescale becomes even shorter. For smaller carbon numbers, the fraction of β -hydroxynitrates in the particles will decrease and the timescale for reaching equilibrium will increase, allowing more time for loss by gas-wall partitioning.

A number of experimental observations also indicate that C_{14} and C_{15} β -hydroxynitrates were essentially all in the particle phase throughout an experiment, so that losses by gas—wall partitioning were negligible. First, the TDPBMS time profile of the m/z 199 ion (normalized to the m/z 149 ion of the nonvolatile DOP to correct for particle wall loss), which is characteristic of both C_{14} β -hydroxynitrate isomers, 5,39 is essentially flat after reaching a maximum within a few minutes of turning off the lights (Figure 6), whereas it would decrease if

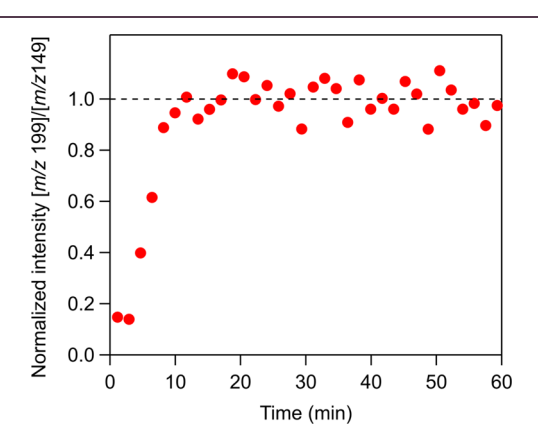


Figure 6. Time profile of the ratio of the intensities of the m/z 199 and 149 ions, which are characteristic of the C_{14} β -hydroxynitrates and DOP, respectively, measured with the TDPBMS in the reaction of 1-tetradecene with OH/NO_x. Data points are 2 min averages scaled by a single factor to achieve an average value of 1.0 after turning off the lights.

evaporation were occurring. Next, the similar yields measured here for C_{14} and C_{15} β -hydroxynitrates in eight experiments (Table 1, discussed below) and in our previous study⁵ for $C_{14}-C_{17}$ β -hydroxynitrates indicate that the fraction of β -hydroxynitrates that partitioned to the chamber walls during the experiments was negligible since otherwise, the yields should increase with increasing carbon number due to

decreasing β -hydroxynitrate vapor pressures and correspondingly smaller losses. And finally, the similar yields measured for C_{15} β -hydroxynitrates in three 6 min experiments (Table 1, expt 5–7) and one in which the lights were only on for 1 min (Table 1, Exp. 8) but at a higher intensity (so about the same amount of SOA was formed) provide additional support for this conclusion since the more rapid increase in the aerosol mass concentration during the 1 min reaction will enhance gasto-particle partitioning and reduce gas-to-wall partitioning.

Loss of β -Hydroxynitrates by Secondary Reactions with OH Radicals. β -Hydroxynitrates can also be lost during the period that the lights are turned on by reaction with OH radicals, which can occur with β -hydroxynitrates in the gas or particle phase. Here, we employ simple equations that apply to the extreme cases in which β -hydroxynitrates exist either entirely in the gas phase or entirely in the particles throughout the reaction. If β -hydroxynitrates are present only in the gas phase when the lights are turned on, then the fraction that reacts with OH radicals during an experiment can be calculated using the equation developed by Atkinson et al. 40 from consecutive reaction rate theory

$$F = (((1 - k_{HN}/k_{Alk})(1 - ([Alk]_t/[Alk]_0)) /(([Alk]_t/Alk]_0)^{k_{HN}/k_{Alk}} - ([Alk]_t/[Alk]_0))) - 1$$
 (6)

where $k_{\rm HN}/k_{\rm Alk}$ is the ratio of the rate constants for the reactions of OH radicals with the β -hydroxynitrate and alkene, and $[{\rm Alk}]_t/[{\rm Alk}]_o$ is the fraction of alkene unreacted. Using rate constants ^{3,14} of $k_{\rm HN}=1.6\times 10^{-11}$ and $k_{\rm Alk}=5.2\times 10^{-11}$ and 0.5 for the fraction of alkene unreacted in the C_{14} 1-alkene reaction (Table S1), we obtain F=0.13. Although not large, this value must overestimate the fraction lost by reactions in the gas phase by more than an order of magnitude since, as discussed above, the β -hydroxynitrates are present almost entirely in particles for most of the reaction. If, for example, 5% of the β -hydroxynitrates remain in the gas phase while the lights are on, then 0.7% (0.05 × 0.13 × 100) will react with OH radicals.

Conversely, if C_{14} β -hydroxynitrates are present only in the particles when the lights are turned on, which should be an accurate assumption for these experiments based on the gas—particle partitioning discussion above, then the fraction that reacts with OH radicals can be calculated using the equation

$$F = 3\gamma c M[OH]t/2d\rho L \tag{7}$$

which is derived from the ratio of the number of reactive collisions that occur between OH radicals and a spherical particle in a given time, ⁴¹ divided by the number of molecules in the particle. The quantities in the equation and the values used here are as follows: $\gamma = 0.5$ is the reactive uptake coefficient, ⁴² $c = 6 \times 10^4$ cm s⁻¹ is the mean thermal speed of OH radicals calculated from kinetic theory, ⁴³ $d = 3 \times 10^{-5}$ cm is the average particle diameter, t = 360 s is the reaction time, $\rho = 1.13$ g cm⁻³ is the particle density, ⁵ M = 273 g mole⁻¹ is the mean molecular weight of SOA molecules taken to be that of C₁₄ β -hydroxynitrates, and $L = 6 \times 10^{23}$ molecules mole⁻¹ is Avogadro's number. The value of [OH] = 3.7×10^7 cm⁻³ for the average concentration of OH radicals was calculated from the first-order kinetics equation

$$[OH] = -\ln([Alk]_t/[Alk]_0)/k_{Alk}t$$
(8)

using values for $[Alk]_t/[Alk]_o$, k_{Alk} , and t given above. The resulting value of F = 0.01 indicates that only $\sim 1\%$ of the β -

Table 1. Yields of β -Hydroxynitrates (β -HN) and SOA Formed from Reactions of 1-Tetradecene (1-TD), 1-Pentadecene (1-PD), 7-Pentadecene (7-PD), and 2-Methyl-1-tetradecene (2M-1-TD) with OH/NO.

			eta -HN molar yiel $\mathrm{d}^{a,b}$			eta -HN molar yield/OH addition a,b		
expt	alkene	SOA mass yield	1H2N	1N2H	total	1H2N	1N2H	total ^b
1	1-TD	0.60	0.089	0.034	0.123	0.125	0.048	0.173
2	1-TD	0.59	0.110	0.026	0.136	0.155	0.037	0.192
3	1-TD	0.62	0.102	0.030	0.132	0.144	0.042	0.186
4	1-TD	0.64	0.080	0.028	0.108	0.113	0.039	0.152
1-4 av		0.61 ± 0.02	0.095 ± 0.01	0.030 ± 0.003	0.125 ± 0.01	0.134 ± 0.02	0.042 ± 0.004	0.176 ± 0.02
5	1-PD	0.57	0.107	0.035	0.142	0.155	0.051	0.206
6	1-PD	0.65	0.089	0.030	0.119	0.129	0.043	0.172
7	1-PD	0.70	0.095	0.034	0.129	0.137	0.049	0.186
8	1-PD	0.62	0.077	0.028	0.105	0.111	0.041	0.152
5-8 av		0.64 ± 0.05	0.092 ± 0.01	0.032 ± 0.003	0.124 ± 0.01	0.133 ± 0.02	0.046 ± 0.005	0.179 ± 0.02
1-8 av		0.62 ± 0.04	0.094 ± 0.01	0.031 ± 0.003	0.124 ± 0.01	0.134 ± 0.02	0.044 ± 0.005	0.177 ± 0.02
9	7-PD	0.27			0.147			0.181
10	2M-1-TD	0.62	0.178	0.029	0.207	0.214	0.035	0.249

[&]quot;Isomer yields could not be measured for the reaction of 7-pentadecene but should be equal. ${}^b\beta$ -HN molar yields divided by the fraction of the reaction that occurs by addition to the double bond.

hydroxynitrates react with OH radicals, and, when combined with the results presented above for possible gas-phase reactions, it indicates that in these experiments, the loss of β -hydroxynitrates by secondary reactions with OH radicals was negligible.

We note that for reactions in which the products of interest do not fully partition to the particle phase (and hence OH reaction losses would be expected to be non-negligible), one can use a kinetics model that couples gas—wall partitioning, gas—particle partitioning, and secondary reactions with OH radicals. The model can employ the gas—wall partitioning parameterization given in Krechmer et al.,³¹ gas—particle partitioning theory,³⁷ vapor pressures estimated using SIMPOL.1,³⁸ measured aerosol mass concentrations, OH radical rate constants taken from the literature or estimated,³ and an average OH radical concentration calculated as described above.

Measured Molar Yields and Branching Ratios for the **Formation of** β **-Hydroxynitrates.** The molar yields of β hydroxynitrates formed from reactions of linear 1-alkenes have been previously shown to increase with increasing carbon number until $\sim C_{14}$, at which point the yields reach a plateau.⁵ The molar yields of alkyl nitrates formed from OH/NO_x reactions of *n*-alkanes exhibit a similar behavior, ²⁰ which is captured in a model developed by Arey et al.¹⁹ This carbon number dependence occurs because as carbon number increases the internal energy released into the β -hydroxyperoxy radical-NO complex by the exothermicity of the reaction can be dispersed among an increasing number of vibrational modes, leading to enhanced stability that allows more time for the intramolecular rearrangement that must occur to form the nitrate group. 18 As a result, the fraction of β -hydroxyperoxy radicals that react with NO to form β -hydroxynitrates (α_3 , α_4) rather than β -hydroxyalkoxy radicals and NO₂ (α_5 , α_6) increases (Scheme 1). Therefore, here we report an average of the β -hydroxynitrate yields from the C_{14} and C_{15} 1-alkenes, which fall on the plateau and should be very nearly equal. The isomer-averaged molar yield (moles β -hydroxynitrate formed divided by the moles 1-alkene reacted) of β -hydroxynitrates for eight experiments was 0.124 \pm 0.01, with yields of 0.094 \pm 0.01 and 0.031 \pm 0.003 for the 1H2N and 1N2H isomers, respectively, where the reported uncertainty is the standard

deviation. These values can be divided by $\alpha_{\rm add}$ to normalize to the fraction of the reaction that occurs by OH radical addition, which is 0.710 for the C_{14} 1-alkenes and 0.691 for the C_{15} 1-alkenes. The resulting OH addition-normalized yields for the 1H2N and 1N2H isomers are 0.134 \pm 0.02 and 0.044 \pm 0.005, respectively, and the isomer-averaged value of $\alpha_{\beta \rm HN} = 0.177 \pm 0.02$, which is equivalent to the average branching ratio for the β -hydroxynitrate formation from the reaction of β -hydroxyperoxy radicals with NO. Values for the C_{14} and C_{15} 1-alkenes agree within measurement uncertainties, and results for all of the experiments are shown in Table 1.

The value of 0.177 for the average branching ratio is 26% higher than the value of 0.140 we measured previously for the $C_{14}-C_{17}$ plateau. This difference can be attributed to the 19% increase in filter collection efficiency obtained here by removing the metal screens in the filter sampler and the 6% lower molar absorptivity determined here for the β -hydroxynitrate calibration standard. Applying these corrections to the branching ratio of Matsunaga and Ziemann gives a value of 0.177 (1.19 \times 1.06 \times 0.140), the same as the value measured here.

The plateau branching ratio of 0.177 can be extrapolated to smaller carbon numbers using the model of Arey et al. 19 for alkyl nitrates by first shifting values by one carbon number to account for the additional heavy atom provided by the O atom in the hydroxyl group⁷ and then scaling all values to the ratio of the plateau branching ratios for β -hydroxynitrates/alkyl nitrates, 0.177/0.292 = 0.61. Model curves for the β hydroxynitrates and alkyl nitrates are shown in Figure 7 over the range of heavy atoms from 3 to 16 (corresponding to C₃- C_{16} for alkyl nitrates and C_2 – C_{15} for β -hydroxynitrates) along with measured values. The smaller branching ratios for β hydroxynitrates compared to those for alkyl nitrates are consistent with the quantum chemical calculations reported by O'Brien et al.,4 which indicated that hydrogen bonding between the hydroxyl and peroxy functional groups in the β hydroxyperoxy radical-NO complex weakens the O-O bond, leading to increased decomposition to the alkoxy radical and NO_2 and therefore lower yields of β -hydroxynitrates relative to

Our results can be compared with those of Teng et al., 7 who measured yields and branching ratios for gas-phase β -

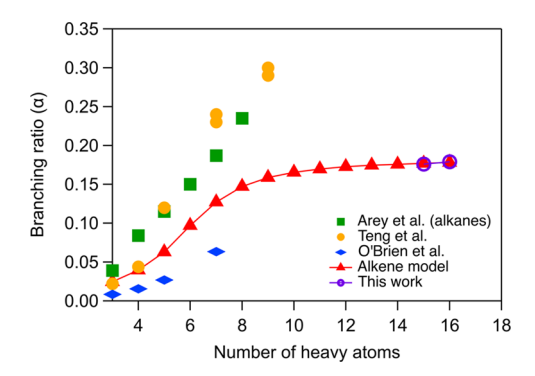


Figure 7. Comparison of measured branching ratios for organic nitrate formation from the reactions of linear alkanes (green squares, Arey et al.¹⁹) and 1-alkenes (yellow circles, Teng et al.; blue diamonds, O'Brien et al.⁴) with OH/NO_x. The values measured in this study are shown as open purple circles, and the red triangles are calculated by scaling the model of Arey et al.¹⁹ to the plateau values measured here, as described in the text.

hydroxynitrates formed from similar reactions of C2-C8 1alkenes in environmental chamber experiments. Products were analyzed using a combination of online GC-CIMS (with the CF₃O⁻ reagent ion) and thermal decomposition-laser-induced fluorescence. The measured branching ratios are also plotted in Figure 7. For the C_4 , C_6 , and C_8 1-alkenes, values are ~85% higher than those determined here from measurements and modeling and ~13% higher than those predicted from the Arey et al. 19 measurements and modeling for alkyl nitrates with the same number of heavy atoms. Also shown in the figure are results of measurements of branching ratios for β -hydroxynitrates measured by O'Brien et al.4 in chamber experiments of C2-C6 1-alkenes using an online GC coupled to a nitratespecific luminol-based NO₂ detector to detect organic nitrates. Modeling by Teng et al. indicates that under the conditions of the O'Brien et al.⁴ experiments O(³P) atoms were formed and reacted with the 1-alkenes, leading to underestimates of the true yields.

Uncertainty Analysis for β -Hydroxynitrate Yields. Because we performed four experiments with 1-tetradecene and four with 1-pentadecene (Table 1) and because the C₁₄ and C_{15} β -hydroxynitrate yields were averaged (since the individual averages were the same within the standard deviations and within the C_{14} - C_{17} plateau region observed by Matsunaga and Ziemann⁵), we can report the standard deviation for β -hydroxynitrate yields and branching ratios across the eight experiments: $Y_{\rm BHN}$ = 0.124 \pm 0.01 and $\alpha_{\rm BHN}$ = 0.177 ± 0.02. However, because we have examined each component of the yield measurement and its associated uncertainty in the previous sections, we can also propagate those uncertainties to obtain an estimate of the total uncertainty in the molar yield. The mathematical operations applied to each measurement to ultimately calculate molar yields consist only of multiplication and division, and therefore, the relative uncertainty for an individual molar yield measurement can be calculated as the square root of the sum of the squares of the relative uncertainty for each measurement

$$\sigma_t = \sqrt{{\sigma_1}^2 + {\sigma_2}^2 + {\sigma_3}^2 \dots}$$
 (9)

where σ_t is the relative uncertainty for the β -hydroxynitrate yield and σ_1^2 , σ_2^2 , σ_3^2 , etc., are the squares of the individual relative uncertainties for each measurement. These values

include the uncertainty across the averaged CO₂ measurements used to calculate chamber volume (1.1%), the uncertainty for the measured filter flow rates used to collect particle-phase β hydroxynitrates (1.3%), the uncertainty from the slope of the line for the DOP calibration used to correct for particle deposition to walls (0.4%), the uncertainty across replicate Tenax samples used to measure the amount of 1-alkene reacted (3.2%), the uncertainty in the microbalance measurements of β -hydroxynitrates used to prepare the HPLC calibration curve (1.1%), and the uncertainty from the slope of the line for the β -hydroxynitrate calibration curve (1.9%). When propagated, the result is a 4.3% relative uncertainty applied to each β hydroxynitrate yield measurement. Note that this calculation does not include uncertainties due to gas-wall partitioning of 1-alkenes or β -hydroxynitrates, or secondary reactions of β hydroxynitrates with OH radicals since we concluded that these were negligible.

Finally, we can report the uncertainty on the average of all eight yields as the standard error of the mean, σ_t/\sqrt{N} , where N is the number of experiments, which can be applied to the isomer-averaged branching ratio as well. The molar yield of β -hydroxynitrates with the propagated uncertainty is 0.124 \pm 0.005, and the branching ratio for β -hydroxynitrate formation is 0.177 \pm 0.008. Because the propagated uncertainty (4.3%) is lower than the reported standard deviation across the eight experiments (10%), we report the experimental standard deviation as the uncertainty.

Pathway-Specific Branching Ratios for the Formation of β -Hydroxynitrates. In a previous study, we used plateau values of OH addition-normalized yields of β -hydroxynitrate isomers measured for the reactions of 1-alkenes, internal alkenes, and 2-methyl-1-alkenes to calculate values of the branching ratios α_1 - α_6 shown in Scheme 1 for each of the three types of radicals formed. This included the branching ratios α_1 and α_2 for the formation of primary, secondary, and tertiary β -hydroxyperoxy radicals and the branching ratios α_3 and α_4 for the subsequent formation of the corresponding primary, secondary, and tertiary β -hydroxynitrates. The values obtained for α_1 and α_2 were 0.50:0.50 for the formation of the two secondary β -hydroxyperoxy radicals in the reactions of internal alkenes, 0.65:0.35 for the formation of the secondary/ primary β -hydroxyperoxy radicals in the reactions of 1-alkenes, and 0.81:0.19 for the formation of the tertiary/primary β hydroxyperoxy radicals in the reactions of 2-methyl-1-alkenes. The values determined for the branching ratios α_3 and α_4 for the formation of primary, secondary, and tertiary β hydroxynitrates were 0.12, 0.15, and 0.25, respectively, with the branching ratios for the formation of the corresponding primary, secondary, and tertiary β -hydroxyalkoxy radicals being one minus these values: 0.88, 0.85, and 0.75.

These values can be recalculated using the results presented here. As discussed above, the OH addition-normalized plateau yields for the 1H2N and 2H1N β -hydroxynitrate isomers formed from the 1-alkene reaction were 0.134 and 0.044, respectively. For the single 7-pentadecene experiment, the isomer-averaged molar yield of β -hydroxynitrates was 0.147 and the OH addition-normalized yield was 0.181. Since there were no distinguishable isomers (the molecule is almost symmetric), we can assume that the values for the individual isomers were the same and so equal to 0.074 and 0.091, respectively. For the single 2-methyl-1-tetradecene experiment, the isomer-averaged molar yield of β -hydroxynitrates was 0.207, the yields for the 1H2N and 1N2H isomers were 0.178

and 0.029, and the corresponding OH addition-normalized yields were 0.249, and 0.214 and 0.035, respectively.

We note that when the OH addition-normalized yields of 0.149 and 0.225 we measured previously for internal alkenes and 2-methyl-1-alkenes are corrected for filter sampling and the difference in molar absorptivity, the values are 0.155 and 0.271, compared to those measured here of 0.181 and 0.249, respectively. These differences of \sim 14 and \sim 9%, respectively, may be due to measurement uncertainties, which are enhanced since only one experiment was conducted for each of these alkenes. However, the lower value for the internal alkenes may also be due in part to the much longer sampling time used in the previous experiments, since these β -hydroxynitrates are more volatile than those formed from the other alkenes. It was not clear then that the yields had reached the plateau, and so some β -hydroxynitrates might have been lost by gas—wall partitioning during filter sampling.

By assuming that the branching ratio for any pathway for forming or reacting a β -hydroxyperoxy radical with NO depends only on whether it is primary, secondary, and tertiary, the measured OH addition-normalized yields for reactions of 1-tetradecene, 1-pentadecene, 7-pentadecene, and 2-methyl-1tetradecene can be used to calculate these branching ratios. The calculations are described in the SI and are similar to those we conducted previously.⁶ The calculations give values for the branching ratios for adding to the 1-carbon and 2carbon in 1-alkenes, internal alkenes, and 2-methyl-1-alkenes of 0.74:0.26 (0.65:0.35), 0.50:0.50 (0.50:0.50), and 0.79:0.21 (0.81:0.19), and branching ratios for forming the β hydroxynitrate from the reaction of a primary, secondary, or tertiary β -hydroxyperoxy radical of 0.17 (0.12), 0.18 (0.15), and 0.27 (0.25), respectively, where values in parentheses were determined previously.⁶ Although the values determined here differ slightly from the previous ones, they again indicate that the branching ratios for the OH radical addition to C=C bonds to form β -hydroxyperoxy radicals, and the reactions of β -hydroxyperoxy radicals with NO to form β -hydroxynitrates, increase in the order primary < secondary < tertiary.

■ CONCLUSIONS

The results of this study demonstrate the large number of factors that must be accounted for when performing quantitative measurements of reaction products in environmental chamber studies. Even for the reactions of simple linear 1-alkenes, the sampling and measurement techniques, synthesis of authentic standards, and losses of precursor compounds and products to chamber walls and secondary reactions make the quantitative determination of product yields and branching ratios challenging. However, by taking inventory of each potential source of error and attempting to minimize its contribution to measurement uncertainty, accurate measurements can be made. Here, we demonstrated this process by measuring the yields and branching ratios for the formation of β -hydroxynitrates from the OH radical-initiated reactions of C_{14} and C_{15} 1-alkenes in the presence of NO_x . Values are ~25% higher than those measured previously,⁵ for reasons that were determined here during our attempts to minimize sources of measurement errors. The isomer-averaged branching ratios are \sim 61% of those determined for alkyl nitrates formed from similar reactions of linear alkanes, ^{19,20} apparently due to a weakening of the O-O bond in the β -hydroxyperoxy radical— NO complex by hydrogen bonding with the hydroxyl group.⁴ When combined with single measurements of the yields of β - hydroxynitrates formed from reactions of an internal alkene and 2-methyl-1-alkene, 7-pentadecene, and 2-methyl-1-tetradecene, the calculated branching ratios for the OH radical addition to C=C bonds to form β -hydroxyperoxy radicals, and the reactions of β -hydroxyperoxy radicals with NO to form β -hydroxynitrates, are shown to increase in the order primary < secondary < tertiary. Results obtained from studies such as this are important for developing quantitative chemical mechanisms for use in models applied to laboratory and field measurements and for gaining a deeper understanding of atmospheric VOC oxidation and SOA formation.

ASSOCIATED CONTENT

Supporting Information

The Supporting Information is available free of charge at https://pubs.acs.org/doi/10.1021/acsearthspace-chem.1c00008.

Experimental conditions for reactions of alkenes with OH/NO_x (Table S1); CO_2 calibration curve (Figure S1); microbalance mass accuracy curve (Figure S2); and calculation of reaction branching ratios from OH addition-normalized yields (PDF)

AUTHOR INFORMATION

Corresponding Author

Paul J. Ziemann — Department of Chemistry, University of Colorado, Boulder, Colorado 80309, United States; Cooperative Institute for Research in Environmental Sciences (CIRES), Boulder, Colorado 80309, United States; orcid.org/0000-0001-7419-0044; Phone: 303-492-9654; Email: paul.ziemann@colorado.edu

Author

Julia G. Bakker-Arkema — Department of Chemistry, University of Colorado, Boulder, Colorado 80309, United States; Cooperative Institute for Research in Environmental Sciences (CIRES), Boulder, Colorado 80309, United States; orcid.org/0000-0002-3120-6058

Complete contact information is available at: https://pubs.acs.org/10.1021/acsearthspacechem.1c00008

Notes

The authors declare no competing financial interest.

ACKNOWLEDGMENTS

This material is based on work supported by the National Science Foundation under grants AGS-1420007 and AGS-1750447.

REFERENCES

- (1) Guenther, A. B.; Jiang, X.; Heald, C. L.; Sakulyanontvittaya, T.; Duhl, T.; Emmons, L. K.; Wang, X. The Model of Emissions of Gases and Aerosols from Nature Version 2.1 (MEGAN2.1): An Extended and Updated Framework for Modeling Biogenic Emissions. *Geosci. Model Dev.* 2012, 5, 1471–1492.
- (2) Huang, G.; Brook, R.; Crippa, M.; Janssens-Maenhout, G.; Schieberle, C.; Dore, C.; Guizzardi, D.; Muntean, M.; Schaaf, E.; Friedrich, R. Speciation of Anthropogenic Emissions of Non-Methane Volatile Organic Compounds: A Global Gridded Data Set for 1970–2012. Atmos. Chem. Phys. 2017, 17, 7683–7701.
- (3) Ziemann, P. J.; Atkinson, R. Kinetics, Products, and Mechanisms of Secondary Organic Aerosol Formation. *Chem. Soc. Rev.* **2012**, *41*, 6582–6605.

- (4) O'Brien, J. M.; Czuba, E.; Hastie, D. R.; Francisco, J. S.; Shepson, P. B. Determination of the Hydroxy Nitrate Yields from the Reaction of C_2 – C_6 Alkenes with OH in the Presence of NO. *J. Phys. Chem. A* **1998**, *102*, 8903–8908.
- (5) Matsunaga, A.; Ziemann, P. J. Yields of β -Hydroxynitrates and Dihydroxynitrates in Aerosol Formed from OH Radical-Initiated Reactions of Linear Alkenes in the Presence of NO_x. *J. Phys. Chem. A* **2009**, *113*, 599–606.
- (6) Matsunaga, A.; Ziemann, P. J. Yields of β -Hydroxynitrates, Dihydroxynitrates, Trihydroxynitrates Formed from OH Radical-Initiated Reactions of 2-Methyl-1-Alkenes. *Proc. Natl. Acad. Sci. U.S.A.* **2010**, *107*, 6664–6669.
- (7) Teng, A. P.; Crounse, J. D.; Lee, L.; St. Clair, J. M.; Cohen, R. C.; Wennberg, P. O. Hydroxy Nitrate Production in the OH-Initiated Oxidation of Alkenes. *Atmos. Chem. Phys.* **2015**, *15*, 4297–4316.
- (8) Wennberg, P. O.; Bates, K. H.; Crounse, J. D.; Dodson, L. G.; McVay, R. C.; Mertens, L. A.; Nguyen, T. B.; Praske, E.; Schwantes, R. H.; Smarte, M. D.; et al. Gas-Phase Reactions of Isoprene and its Major Oxidation Products. *Chem. Rev.* **2018**, *118*, 3337–3390.
- (9) Xu, L.; Møller, K. H.; Crounse, J. D.; Otkjær, R. V.; Kjaergaard, H. G.; Wennberg, P. O. Unimolecular Reactions of Peroxy Radicals Formed in the Oxidation of α -Pinene and β -Pinene by Hydroxyl Radicals. *J. Phys. Chem. A* **2019**, *123*, 1661–1674.
- (10) Lohmann, U.; Feichter, J. Global Indirect Aerosol Effects: A Review. Atmos. Chem. Phys. 2005, 5, 715–737.
- (11) Pöschl, U. Atmospheric Aerosols: Composition, Transformation, Climate and Health Effects. *Angew. Chem., Int. Ed.* **2005**, 44, 7520–7540.
- (12) Peeters, J.; Nguyen, T. L.; Vereecken, L. HO_x Radical Regeneration in the Oxidation of Isoprene. *Phys. Chem. Chem. Phys.* **2009**, *11*, 5935–5939.
- (13) Perring, A. E.; Puesede, S. E.; Cohen, R. C. An Observational Perspective on the Atmospheric Impacts of Alkyl and Multifunctional Nitrates on Ozone and Secondary Organic Aerosol. *Chem. Rev.* **2013**, *113*, 5848–5870.
- (14) Nishino, N.; Arey, J.; Atkinson, R. Rate Constants for the Gas-Phase Reactions of OH Radicals with a Series of C_6 - C_{14} Alkenes at 299 \pm 2 K. J. Phys. Chem. A **2009**, 113, 852–857.
- (15) Orlando, J. J.; Tyndall, G. S. Laboratory Studies of Organic Peroxy Radical Chemistry: An Overview with Emphasis on Recent Issues of Atmospheric Significance. *Chem. Soc. Rev.* **2012**, *41*, 6294–6317.
- (16) Atkinson, R. Gas-Phase Tropospheric Chemistry of Volatile Organic Compounds: 1. Alkanes and Alkenes. *J. Phys. Chem. Ref. Data* 1997, 26, 215–290.
- (17) Atkinson, R. Rate Constants for the Atmospheric Reactions of Alkoxy Radicals: An Updated Estimation Method. *Atmos. Environ.* **2007**, *41*, 8468–8485.
- (18) Zhang, J.; Dransfield, T.; Donahue, N. M. On the Mechanism for Nitrate Formation via the Peroxy Radical + NO Reaction. *J. Phys. Chem. A* **2004**, *108*, 9082.
- (19) Arey, J.; Aschmann, S. M.; Kwok, E. S. C.; Atkinson, R. Alkyl Nitrate, Hydroxyalkyl Nitrate, and Hydroxycarbonyl Formation from the NO_x –Air Photooxidations of C_5 – C_8 n-Alkanes. J. Phys. Chem. A **2001**, 105, 1020–1027.
- (20) Yeh, G. K.; Ziemann, P. J. Alkyl Nitrate Formation from the Reactions of C₈–C₁₄ n-Alkanes with OH Radicals in the Presence of NOx: Measured Yields with Essential Correctins for Gas–Wall Partitioning. *J. Phys. Chem. A* **2014**, *118*, 8147–8157.
- (21) Taylor, W. D.; Allston, T. D.; Moscato, M. J.; Fazekas, G. B.; Kozlowski, R.; Takacs, G. A. Atmospheric Photodissociation Lifetimes for Nitromethane, Methyl Nitrite, and Methyl Nitrate. *Int. J. Chem. Kinet.* **1980**, *12*, 231–240.
- (22) Finewax, Z.; Jimenez, J. L.; Ziemann, P. J. Development and Application of a Low-Cost Vaporizer for Rapid, Quantitative, In Situ Addition of Organic Gases and Particles to an Environmental Chamber. *Aerosol Sci. Technol.* **2020**, *54*, 1567–1578.

- (23) Raff, J. D.; Finlayson-Pitts, B. J. Hydroxyl Radical Quantum Yields from Isopropyl Nitrite Photolysis in Air. *Environ. Sci. Technol.* **2010**, *44*, 8150–8155.
- (24) Docherty, K. S.; Ziemann, P. J. Effects of Stabilized Criegee Intermediate and OH Radical Scavengers on Aerosol Formation from Reactions of β -Pinene with O₃. Aerosol. Sci. Technol. **2003**, 37, 877–891.
- (25) Tobias, H. J.; Kooiman, P. M.; Docherty, K. S.; Ziemann, P. J. Real-Time Chemical Analysis of Organic Aerosols Using a Thermal Desorption Particle Beam Mass Spectrometer. *Aerosol Sci. Technol.* **2000**, 33, 170–190.
- (26) Hallquist, M.; Wenger, J. C.; Baltensperger, U.; Rudich, Y.; Simpson, D.; Claeys, M.; Dommen, J.; Donahue, N. M.; George, C.; Goldstein, A. H.; et al. The Formation, Properties, and Impact of Secondary Organic Aerosol: Current and Emerging Issues. *Atmos. Chem. Phys.* **2009**, *9*, 5155–5236.
- (27) Pagonis, D.; Krechmer, J. E.; de Gouw, J.; Jimenez, J. L.; Ziemann, P. J. Effects of Gas-Wall Partitioning in Teflon Tubing and Instrumentation on Time-Resolved Measurements of Gas-Phase Organic Compounds. *Atmos. Meas. Tech.* **2017**, *10*, 4687–4696.
- (28) Matsunaga, A.; Ziemann, P. J. Gas-Wall Partitioning of Organic Compounds in a Teflon Film Chamber and Potential Effects on Reaction Product and Aerosol Yield Measurements. *Aerosol Sci. Technol.* **2010**, *44*, 881–892.
- (29) Yeh, G. K.; Ziemann, P. J. Gas-Wall Partitioning of Oxygenated Organic Compounds: Measurements, Structure— Activity Relationships, and Correlation with Gas Chromatographic Retention Factor. *Aerosol Sci. Tech.* **2015**, *49*, 727–738.
- (30) Zhang, X.; Schwantes, R. H.; McVay, R. C.; Lignell, H.; Coggon, M. M.; Flagan, R. C.; Seinfeld, J. H. Vapor Wall Deposition in Teflon Chambers. *Atmos. Chem. Phys.* **2015**, *15*, 4197–4214.
- (31) Krechmer, J. E.; Pagonis, D.; Ziemann, P. J.; Jimenez, J. L. Quantification of Gas-Wall Partitioning in Teflon Environmental Chambers using Rapid Bursts of Low-Volatility Oxidized Species Generated in Situ. *Environ. Sci. Technol.* **2016**, *50*, 5757–5765.
- (32) Hinds, W. C. Aerosol Technology: Properties, Behavior, and Measurement of Airborne Particles; John Wiley & Sons: New York, 1982.
- (33) Docherty, K. S.; Ziemann, P. J. Reaction of Oleic Acid Particles with NO₃ Radicals: Products, Mechanism, and Implications for Radical-Initiated Organic Aerosol Oxidation. *J. Phys. Chem. A* **2006**, 110, 3567–3577.
- (34) Aimanant, S.; Ziemann, P. J. Development of Spectrophotometric Methods for the Analysis of Functional Groups in Oxidized Organic Aerosol. *Aerosol Sci. Technol.* **2013**, *47*, 581–591.
- (35) Wang, N.; Jorga, S. D.; Pierce, J. R.; Donahue, N. M.; Pandis, S. N. Particle Wall-Loss Correction Methods in Smog Chamber Experiments. *Atmos. Meas. Tech.* **2018**, *11*, 6577–6588.
- (36) Wiedensohler, A.; Weisner, A.; Weinhold, K.; Birmili, W.; Hermann, M.; Merkel, M.; Müller, T.; Pfeifer, S.; Schmidt, A.; Wehner, B.; Tuch, T.; et al. Mobility Particle Size Spectrometers: Calibration Procedures and Measurement Uncertainties. *Aerosol Sci. Technol.* **2018**, *52*, 146–164.
- (37) Pankow, J. F. An Absorption Model of the Gas/Aerosol Partitioning of Organic Compounds in the Atmosphere. *Atmos. Environ.* **1994**, 28, 185–188.
- (38) Pankow, J. F.; Asher, W. E. SIMPOL.1: A Simple Group Contribution Method for Predicting Vapor Pressures and Enthalpies of Vaporization of Multifunctional Organic Compounds. *Atmos. Chem. Phys.* **2008**, *8*, 2773–2796.
- (39) Matsunaga, A.; Docherty, K. S.; Lim, Y. B.; Ziemann, P. J. Composition and Yields of Secondary Organic Aerosol Formed from OH Radical-Initiated Reactions of Linear Alkenes in the Presence of NO_x: Modeling and Measurements. *Atmos. Environ.* **2009**, *43*, 1349–1357.
- (40) Atkinson, R.; Aschmann, S. M.; Carter, W. P. L.; Winer, A. M.; Pitts, J. N., Jr. Alkyl Nitrate Formation from the Nitrogen Oxide (NO_x)-Air Photooxidations of C_2-C_8 *n*-Alkanes. *J. Phys. Chem. A* **1982**, *86*, 4563–4569.

- (41) Ravishankara, A. R. Heterogeneous and Multiphase Chemistry in the Troposphere. *Science.* **199**7, 276, 1058–1065. (42) Che, D. L.; Smith, J. D.; Leone, S. R.; Ahmed, M.; Wilson, K. R.
- (42) Che, D. L.; Smith, J. D.; Leone, S. R.; Ahmed, M.; Wilson, K. R. Quantifying the Reactive Uptake of OH by Organic Aerosols in a Continuous Flow Stirred Tank Reactor. *Phys. Chem. Chem. Phys.* **2009**, *11*, 7885–7895.
- (43) Adamson, A. W. A Textbook of Physical Chemistry, 2nd ed.; Academic Press: New York, 1979.

Supporting Information

Minimizing Error in Measured Yields of Particle-Phase Products formed in Environmental Chamber Reactions: Revisiting the Yields of β -Hydroxynitrates Formed from 1-Alkene + OH/NO_x Reactions

Julia G. Bakker-Arkema^{†,‡}, Paul J. Ziemann^{†,‡,*}

- † Cooperative Institute for Research in Environmental Sciences (CIRES), Boulder, Colorado 80309, United States
- ‡ Department of Chemistry, University of Colorado, Boulder, Colorado 80309, United States

Abstract. Experimental conditions for reactions of alkenes with OH/NO_x (Table S1); CO₂ calibration curve (Figure S1). Microbalance mass accuracy curve (Figure S2). Calculation of reaction branching ratios from OH addition-normalized yields.

Table S1. Experimental conditions for reactions of 1-tetradecene (1-TD), 1-pentadecene (1-PD), 7-pentadecene (7-PD), and 2-methyl-1-tetradecene (2M-1-TD) with OH/NO_x .

		Chamber	Lights	Alken	Particle		
Exp.	Alkene	volume (L)	(min)	Fraction	molecules $cm^{-3} \times 10^{13}$	wall loss (%)	
1	1-TD	7640	6	0.51	1.11	5.1	
2	1-TD	7550	6	0.52	1.14	2.1	
3	1-TD	7060	6	0.44	1.03	7.0	
4	1-TD	6370	6	0.38	0.99	3.4	
5	1-PD	6700	6	0.61	1.47	7.1	
6	1-PD	7510	6	0.54	1.20	6.4	
7	1-PD	6390	6	0.42	1.07	4.4	
8	1-PD	6280	1	0.40	0.81	4.5	
9	7-PD	6160	6	0.56	1.32	3.6	
10	2M-1-TD	6380	6	0.64	1.45	5.1	

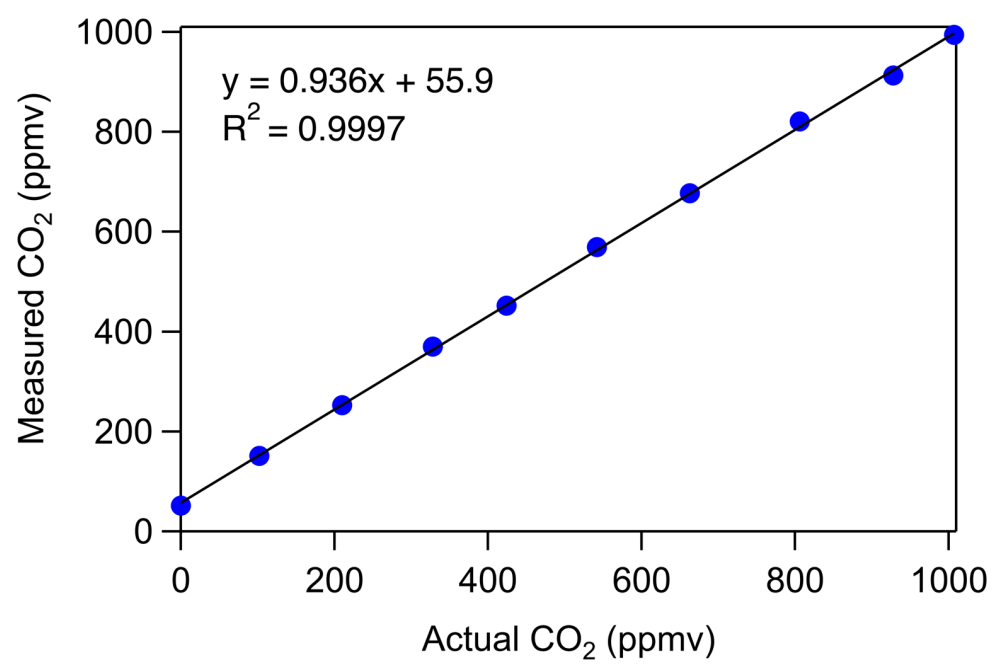


Figure S1. CO₂ probe calibration curve.

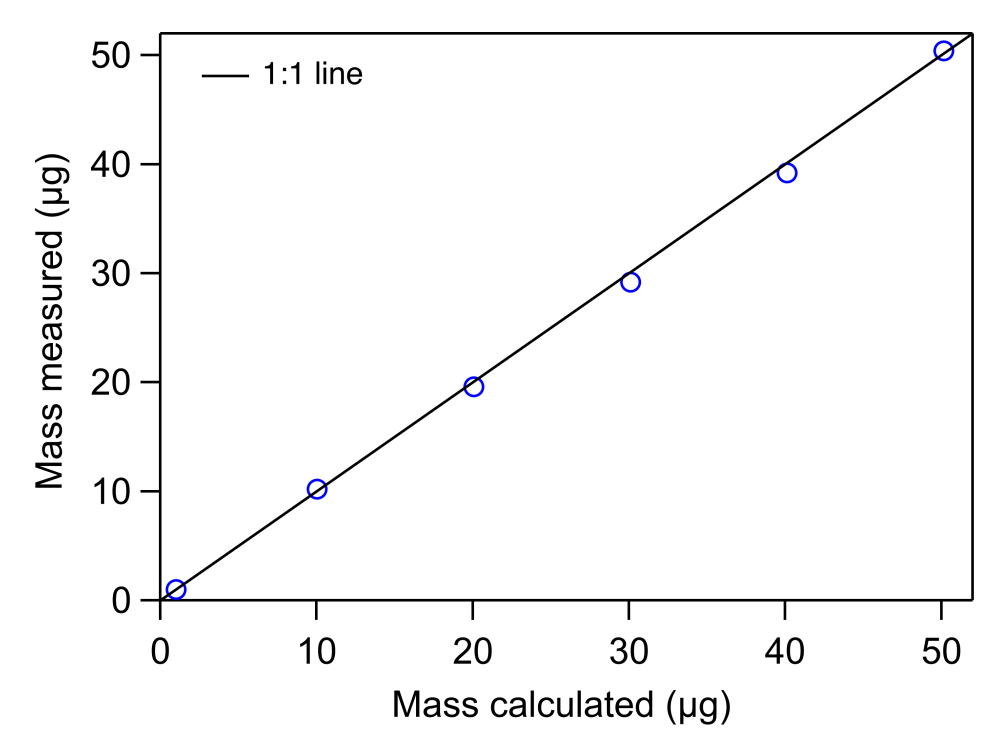


Figure S2. Comparison of microbalance mass measurements and known deposited masses of DOS. The 1:1 line is drawn to demonstrate the agreement between the values, and thus the mass accuracy of the microbalance.

Calculation of Reaction Branching Ratios from OH Addition-Normalized Yields

As shown in Scheme 1, the OH addition-normalized yield, Y, of a β -hydroxynitrate isomer is equal to the product of the branching ratios along the pathway by which it is formed. For the 1H2N and 1N2H isomers this means $Y_{1H2N} = \alpha_1 \times \alpha_3$ and $Y_{2H1N} = \alpha_2 \times \alpha_4$. For the reactions of internal alkenes the two β -hydroxyperoxy radicals that are formed are both secondary, for 1-alkenes they are secondary and primary, and for 2-methyl-1-alkenes they are tertiary and primary. The branching ratios in the equations below are therefore labelled P, S, and T for primary, secondary, and tertiary β -hydroxyperoxy radicals, respectively. Assuming that the branching ratio for any pathway depends only on whether the β -hydroxyperoxy radical that is being formed or is reacting with NO is primary, secondary, and tertiary, the measured OH addition-normalized yields for reactions of the 1-alkenes, internal alkenes, and 2-methyl-1-alkenes can be used to calculate branching ratios for the reaction pathways.

OH Addition-Normalized Yields

1-Alkenes: $Y_{1H2N} = 0.134$, $Y_{2H1N} = 0.044$

Internal Alkenes: $Y_{1H2N} = 0.091$, $Y_{2H1N} = 0.091$

2-Methyl-1-Alkenes: $Y_{1H2N} = 0.214$, $Y_{2H1N} = 0.035$

Internal Alkenes

 $Y_{1H2N} = \alpha_{1S} \times \alpha_{3S}$

 $Y_{2H1N} = \alpha_{2S} \times \alpha_{4S}$

 $\alpha_{1S} = 0.5$

 $\alpha_{2S} = 0.5$

 $\alpha_{3S} = Y_{1H2N}/\alpha_{1S} = 0.091/0.5 = 0.18$

 $\alpha_{4S} = Y_{2H1N}/\alpha_{2S} = 0.091/0.5 = 0.18$

 $\alpha_{5S} = 1 - \alpha_{3S} = 1 - 0.18 = 0.82$

 $\alpha_{6S} = 1 - \alpha_{4S} = 1 - 0.18 = 0.82$

1-Alkenes:

 $Y_{1H2N} = \alpha_{1S} \times \alpha_{3S}$

 $Y_{2H1N} = \alpha_{2P} \times \alpha_{4P}$

 $\alpha_{1S} = Y_{1H2N}/\alpha_{3S} = 0.134/0.18 = 0.74$

 $\alpha_{2P} = 1 - \alpha_{1S} = 1 - 0.74 = 0.26$

 $\alpha_{4P} = Y_{2H1N} = 0.044/0.26 = 0.17$

 $\alpha_{6P} = 1 - \alpha_{4P} = 1 - 0.17 = 0.83$

2-Methyl-1-Alkenes:

$$Y_{1H2N} = \alpha_{1T} \times \alpha_{3T}$$

$$Y_{2H1N} = \alpha_{2P} \times \alpha_{4P}$$

$$\alpha_{2P} = Y_{2H1N}/\alpha_{4P} = 0.035/0.17 = 0.21$$

$$\alpha_{1T} = 1 - \alpha_{2P} = 1 - 0.21 = 0.79$$

$$\alpha_{3T} = Y_{1H2N}/\alpha_{1T} = 0.214/0.79 = 0.27$$

These calculations give the following values for the branching ratios for adding to the 1-carbon and 2-carbon in 1-alkenes, internal alkenes, and 2-methyl-1-alkenes of 0.74:0.26, 0.50:0.50, and 0.79:0.21, respectively; and branching ratios for forming the β -hydroxynitrate and β -hydroxyalkoxy radical from the reaction of a primary, secondary, and tertiary β -hydroxyperoxy radical are 0.17:0.83, 0.18:0.82, and 0.27:0.73.